

Coexistence of Dirac-Cone States and Superconductivity in Iron Pnictide $\text{Ba}(\text{Fe}_{1-x}\text{Ru}_x\text{As})_2$

Y. Tanabe^{1,*}, K. K. Huynh², S. Heguri², G. Mu², T. Urata², J. Xu¹, R. Nouchi¹, N. Mitoma², and K. Tanigaki^{1,2†}

¹WPI-Advanced Institutes of Materials Research, Tohoku University, Aoba, Aramaki, Aoba-ku, Sendai, 980-8578, Japan and

²Department of Physics, Graduate School of Science, Tohoku University, Aoba, Aramaki, Aoba-ku, Sendai, 980-8578, Japan

(Dated: September 22, 2021)

The Ru doping effect on the Dirac cone states is investigated in iron pnictide superconductors $\text{Ba}(\text{Fe}_{1-x}\text{Ru}_x\text{As})_2$ using the transverse magnetoresistance (MR) measurements as a function of temperature. The linear development of MR against magnetic field B is observed for $x = 0 - 0.244$ at low temperatures below the antiferromagnetic transition. The B -linear MR is interpreted in terms of the quantum limit of the Dirac cone states by using the model proposed by Abrikosov. An intriguing evidence is shown that the Dirac cone state persists on the electronic phase diagram where the antiferromagnetism and the superconductivity coexist.

PACS numbers: 74.70.Xa, 74.25.Dw, 72.15.Gd, 75.47.-m

Despite a quite large energy scale for the pairing interaction attributed to the exchange interaction J between Cu spins (~ 2000 K), the small superfluid density and short coherence length of high- T_c cuprates can cause bulk superconducting (SC) state to break down due to the phase fluctuation [1, 2]. In order to realize the bulk SC state at the temperature as high as the pairing energy, the coherency of the Cooper paired electronic states must be enhanced. In the case of a two-dimensional Pb granular system, it has been shown that deposition of Ag on a Pb film enhances intergranular interactions, resulting in the immediate development of a bulk SC state [3]. In high- T_c cuprates, a similar increase in the bulk T_c has been reported for a bilayer film comprised of underdoped $\text{La}_{2-x}\text{Sr}_x\text{CuO}_4$ coated with heavily overdoped metallic $\text{La}_{2-x}\text{Sr}_x\text{CuO}_4$ [4]. It has been proposed that the superconducting domains, which occur in the Fermi liquid states despite they are in fermiologic or nonfermiologic, form one after another as the carrier concentration increases and that coherent bulk SC occurs via Josephson coupling or proximity effects. Thus, Fermi surfaces with high mobility behind Cooper paired electronic states are essential to realize a robust bulk SC state. From a physics viewpoint, the coexistence of highly mobile carriers and superconductivity is important for achieving high- T_c superconductors, and the recent discovery of Dirac cone states in the another high- T_c material iron pnictide superconductors provide a good research stage to study this idea. The Dirac cone state is a novel electronic state with ideal massless fermion character. It has been theoretically predicted to exist in iron pnictide superconductors via special band folding below the antiferromagnetic transition temperature [5–7] and experimentally confirmed in $\text{Ba}(\text{FeAs})_2$ [8–10].

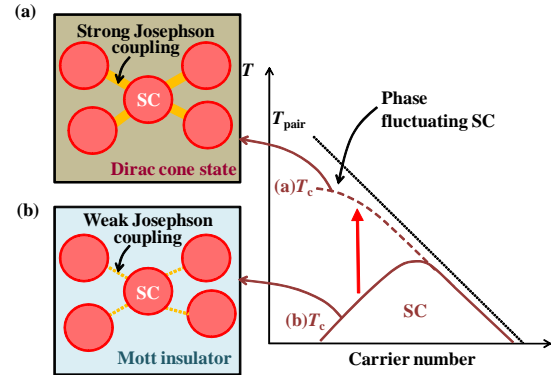


FIG. 1: (color online) Concept of electronic phase diagram in high temperature superconductor (a) with Dirac cone states (b) with the Mott insulator. The strong Josephson coupling of SC islands due to the high mobility state of the Dirac cone immediately develops the bulk superconductivity in (a), while the bulk T_c is suppressed by the strong thermal fluctuation effect due to the weak coupling of SC islands in the insulating background in (b).

There are many reports showing that antiferromagnetic phase survives in iron pnictide superconductors in the underdoped regime of the electronic phase diagram, where T_c increases with an increase in concentration of substituents [11–14]. It has been reported recently that an inhomogeneous microscopic phase occurs between the superconducting phase and the magnetically ordered one in the case of $\text{Ba}_{1-x}\text{K}_x\text{Fe}_2\text{As}_2$ [11, 12]. In addition, the microscopic coexistence of antiferromagnetism and superconductivity in $\text{Ba}(\text{Fe}_{1-x}\text{Co}_x\text{As})_2$ has been suggested [13]. Consequently, highly mobile carriers in the Dirac cone states behind the Cooper paired electronic states in parabolic bands are thought to enhance the coherency of the Cooper pairs via a scattering process (Fig. 1).

We investigated this intriguing electronic states using a Ru substituted pnictide, $\text{Ba}(\text{Fe}_{1-x}\text{Ru}_x\text{As})_2$, so that

*Corresponding author: youichi@sspns.phys.tohoku.ac.jp

†Corresponding author: tanigaki@sspns.phys.tohoku.ac.jp

$x(\text{Ru})$	0	0.0022	0.0051	0.102	0.150	0.190	0.244
$a(\text{\AA})$	3.962	3.962	3.964	3.974	3.980	3.990	3.993
$c(\text{\AA})$	13.02	13.01	12.99	12.96	12.92	12.90	12.86
$T_s(\text{K})$	137.2	131.6	122.5	99.1	83.9	63.7	46.5
$T_c^{\text{onset}}(\text{K})$	-	-	-	-	22.0	21.4	20.0
$T_c(\text{K})$	-	-	-	-	-	-	11.5

TABLE I: The Ru concentration x , the lattice constant, the structure and the magnetic transition temperature T_s , the onset and the middle of the superconducting transition temperature T_c^{onset} and T_c for $\text{Ba}(\text{Fe}_{1-x}\text{Ru}_x\text{As})_2$ single crystals.

the Dirac cone states remained at high concentrations of the substituent. Theoretically, it has been predicted that nonmagnetic impurities do not affect the Dirac cone states, whereas magnetic impurities destroy it [15]. Recent studies on the Nernst effect in $\text{Eu}(\text{Fe}_{1-x}\text{Co}_x\text{As})_2$ and magnetotransport in $\text{Ba}(\text{Fe}_{1-x}\text{TM}_x\text{As})_2$ (TM = Co, Ni, Cu) indicate that the influence of the Dirac fermion on electronic transport is greatly suppressed by substitution with magnetic impurities [16, 17]. Because the Ru 4d orbital is isoelectronic to the Fe 3d orbital, substitution with Ru should not disturb the Dirac cone state [14, 18]. Therefore, we thought that $\text{Ba}(\text{Fe}_{1-x}\text{Ru}_x\text{As})_2$ was an ideal system for exploring the coexistence of superconductivity and Dirac cone states. We showed that, by applying the transverse MR as a function of magnetic field (B) and temperature (T), the Dirac cone state persists in the underdoped regime of $\text{Ba}(\text{Fe}_{1-x}\text{Ru}_x\text{As})_2$ and coexists with the superconductive phase.

Single crystal of $\text{Ba}(\text{Fe}_{1-x}\text{Ru}_x\text{As})_2$ were grown by the flux method using the FeAs flux. Details were described in elsewhere [18]. The qualities of single crystals were checked by the synchrotron X-ray diffraction measurements at the beam line BL02B2, SPring-8. Electrical resistivity ρ measurements were also carried out using the four-probe method to check the quality of the samples. B dependence of the in-plane transverse MR measurements were carried out using the 4 probe methods in $-9 \text{ T} \leq B \leq 9 \text{ T}$ at various fixed temperatures $2 \text{ K} \leq T \leq 150 \text{ K}$.

The Ru concentration (x), the crystal lattice constants, the structure and magnetic transition temperature (T_s), and the onset and the midpoint of the SC transition temperature (T_c^{onset} and T_c , respectively) for $\text{Ba}(\text{Fe}_{1-x}\text{Ru}_x\text{As})_2$ single crystals are listed in Table 1. The value of x for $\text{Ba}(\text{Fe}_{1-x}\text{Ru}_x\text{As})_2$ was determined by employing the relationship between the c -axis lattice constant and x , as previously reported. The values of T_s were determined from the derivatives of the temperature dependences of ρ . Details are described elsewhere [18].

The B dependence of MR for $\text{Ba}(\text{Fe}_{1-x}\text{Ru}_x\text{As})_2$ with $x = 0.190$ at 20 K is shown in Fig. 2(a). The evolution of MR as a function of B is convex in the low- B regime. The T dependence of the resistivity ρ shows a large drop below 21.4 K due to the SC transition. The convex curvature of MR suggests that a crossover occurs from an SC state at low B to a normal state at high B . In order

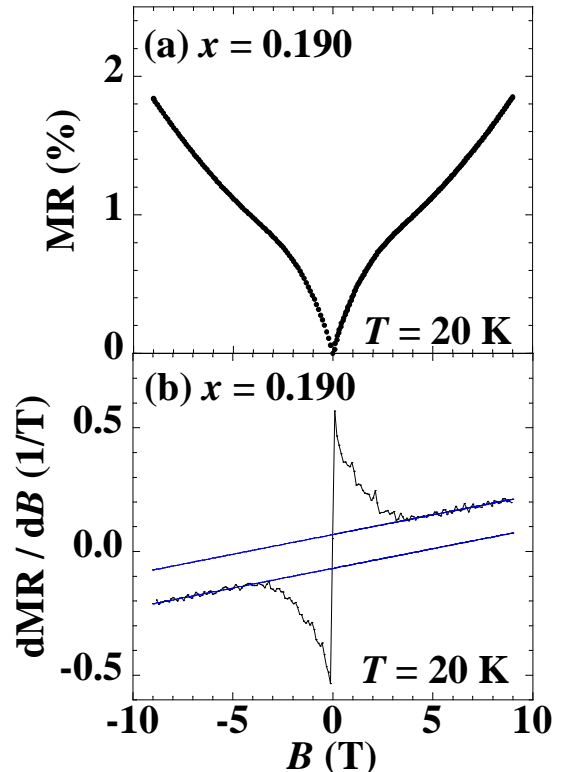


FIG. 2: (color online) (a) Magnetic field (B) dependence of the magnetoresistance (MR) for $\text{Ba}(\text{Fe}_{1-x}\text{Ru}_x\text{As})_2$ with $x = 0.190$ at 20 K. (b) The B derivative of MR for $x = 0.190$. The blue lines were fitted with dMR/dB above $|B| = 4 \text{ T}$.

to clarify the gradient of MR in the normal state, the B dependence of the derivative of MR, dMR/dB , for $x = 0.190$ is plotted in Fig. 2(b). A decrease in dMR/dB was observed in a low B , and then it increased above 4 T. In a high B , dMR/dB became saturated. In fact, the extrapolated line of dMR/dB above $|\pm 4\text{T}|$ shown in Fig. 2(b) deviated from the ideal value of $\text{dMR}/\text{dB} = 0$ under $B = 0 \text{ T}$, indicating that the MR cannot be described as $\text{MR} \propto B^2$, which is the conventional MR behavior for metals in the low B regime, but can be described as $\text{MR} \propto B$ in the Dirac cone states in the high B regime.

The B dependences of MR and dMR/dB for $\text{Ba}(\text{Fe}_{1-x}\text{Ru}_x\text{As})_2$ for various x at 2 K are shown in Figs. 3(a) and (b). For $x = 0.150$ - 0.244 , where the SC transition is observed below 20-22 K, the data at 22 K are shown in Figs. 3(a) and (b). For $x = 0$, MR developed linearly with B , and dMR/dB saturated above 2 T. The values of MR decreased with an increase in x . As x increased, $\text{dMR}/\text{dB} \propto B$ in a low B , and it saturated in a high B for $x = 0$ - 0.150 . We defined the critical magnetic field B^* as the intercept point of the straight lines for $\text{dMR}/\text{dB} \propto B$ in the low B regime and the one in the high B regime where dMR/dB saturates. Above $x = 0.150$, dMR/dB deviated from a straight line with B in the high B regime, as shown for $x = 0.190$ and 0.244

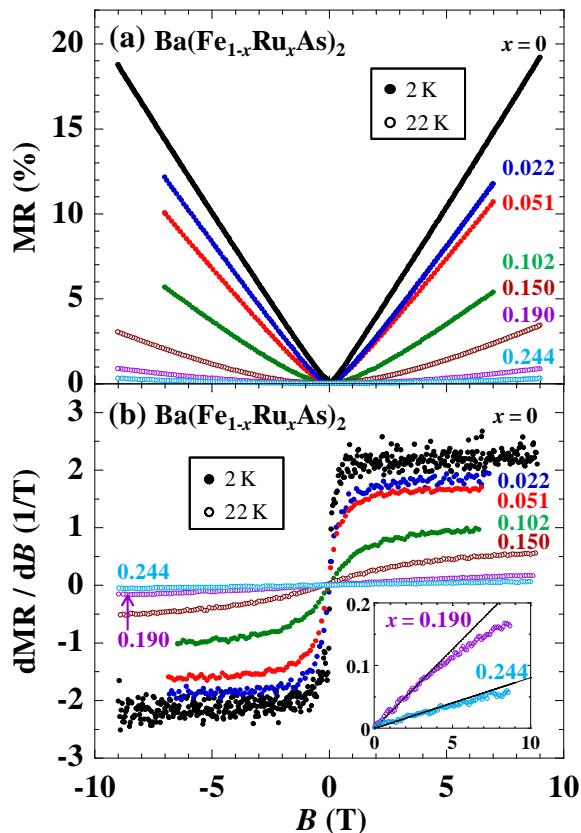


FIG. 3: (color online) (a) Magnetic field (B) dependence of the magnetoresistance (MR) for $\text{Ba}(\text{Fe}_{1-x}\text{Ru}_x\text{As})_2$ with $x = 0-0.150$ at 2 K (close circle) and $x = 0.150-0.244$ at 22 K (open circles). (b) B derivative of MR for $\text{Ba}(\text{Fe}_{1-x}\text{Ru}_x\text{As})_2$ with $x = 0-0.150$ at 2 K (open circle) and $x = 0.150-0.244$ at 22 K (closed circle). Inset of (b) shows a magnified plot of the B derivative of MR for $x = 0.190$ and 0.244. Solid lines represent linear fittings in the semiclassical region.

in the inset of Fig. 3(b).

In order to analyze the data, we employed a theoretical model proposed by Abrikosov [19]. The energy splitting between 0th and 1st Landau levels in the Dirac cone states is described in Eq. (1).

$$\Delta_{\text{LL}} = \pm v_{\text{F}} \sqrt{2e\hbar B} \quad (1)$$

$$B^* = (1/2e\hbar v_{\text{F}}^2)(E_{\text{F}} + k_{\text{B}}T)^2 \quad (2)$$

In the quantum limit, all carriers occupy the 0th Landau level, and Δ_{LL} becomes larger than both the Fermi energy (E_{F}) and the thermal fluctuations at a finite temperature ($k_{\text{B}}T$). In this case, MR is not described using the semiclassical equation $\text{MR} \sim B^2$ but using $\text{MR} \sim (N_{\text{i}}/en_{\text{D}})B$, where N_{i} is the number of impurities and n_{D} is the number of carriers. For a conventional parabolic band, a linearly B -dependent MR can be observed in the quantum limit. However, the energy splitting of the Landau levels for a conventional parabolic band is described by $\Delta_{\text{LL}} = e\hbar B/m^*$ and the evolution of Δ_{LL} with in-

creasing B is much slower than that for the Dirac cone. Consequently, it is not possible to observe quantum limit behavior for the parabolic bands for $\text{Ba}(\text{Fe}_{1-x}\text{Ru}_x\text{As})_2$ below 9 T.

Figure 4(a) shows the temperature dependence of B^* as a function of T^2 . For $x = 0.150$, B^* was estimated above 22 K because the temperature dependence of ρ drops due to the SC transition below 22 K, as explained earlier. The values of B^* for $x = 0.190$ and 0.244 were not estimated for accuracy because dMR/dB was not sufficiently saturated. The B^* values increased monotonically with T^2 for $x = 0-0.150$. At $B = B^*$, Δ_{LL} can be expressed as the sum of E_{F} and $k_{\text{B}}T$, as shown in Eq. (2). The curves for each x fitted with B^* as a function of T are shown as solid lines in Fig. 4(a), and they agree with Eq. (2).

The linealy B -dependent MRs for $\text{Ba}(\text{Fe}_{1-x}\text{Ru}_x\text{As})_2$ with $x = 0-0.244$ are consistent with the quantum limit behavior of MR in a Dirac cone state [10]. Moreover, the temperature dependence of the estimated B^* s for $x = 0-0.150$ can be described using Eq. (2), which is based on the Abrikosov model, as described earlier. Therefore, the Dirac cone states remain after substitution with Ru and are present in the electronic phase diagram where both antiferromagnetism and superconductivity occur at the same time. We estimated both E_{F} and v_{F} using the value of B^* and plotted them as a function of x in Figs. 4(b) and (c).

E_{F} increased with an increased in x , whereas v_{F} slightly decreased with an increase in x . The results indicated that the Ru 4d orbitals caused a larger extension of the wave function than the Fe 3d orbitals did. The on-site Coulomb repulsion (U) becomes smaller, and the bandwidth (W) becomes larger to modify the band reconstruction, influencing the band folding and, thus the Dirac cone states. It is noted here that only the dominant terms from the Dirac cone states with higher mobilities affect MR. Density functional theory calculations suggest that substitution with Ru does not increase the number of carriers but does increase the bandwidth of the Fe 3d orbital via hybridization with the Ru 4d orbital, which has a larger spacial distribution of electrons [20]. Experimentally, ARPES suggests that band renormalization occurs in the overdoped regime of $\text{Ba}(\text{Fe}_{1-x}\text{Ru}_x\text{As})_2$ [21], and thermoelectronic power measurements suggest that the Fermi surface topology changes in $x = 0.07$ and 0.30 [22]. In other words, the increase in E_{F} that we observed above $x = 0.051$ may be due to the change in the Fermi surface topology or band renormalization effects. To the best of our knowledge, there are no reports on the vortex liquid phase as well as the SC fluctuations at temperatures well above the bulk T_{c} [16, 23] for iron pnictide superconductors, although they are important characteristics of high- T_{c} cuprates [24]. In the present experiments, the Dirac cone states remain after substitution with Ru and coexist with superconductivity at low concentrations of Ru. This suggests that the domains made by Cooper paired electrons are more coherent due

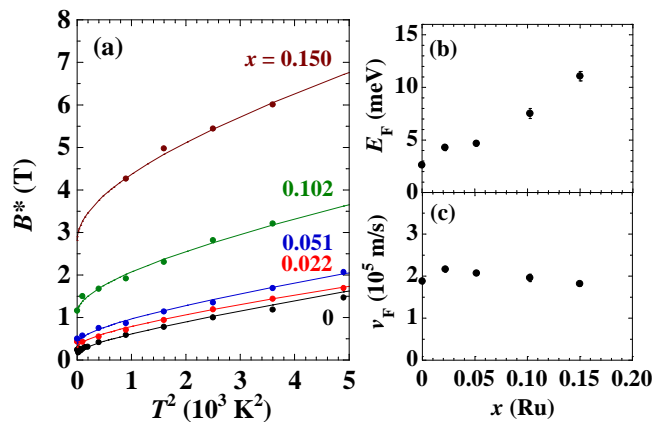


FIG. 4: (color online) (a) B^* vs. T^2 plot for $\text{Ba}(\text{Fe}_{1-x}\text{Ru}_x\text{As})_2$ with $x = 0-0.150$. The solid lines were fitted using $B^* = (1/2e\hbar v_F^2)(E_F + k_B T)^2$. The x dependence of (b) E_F and (c) v_F for $x = 0-0.150$.

to the high mobility of the Dirac cone states. More detailed calculations are needed to explain the electronic phase diagram of $\text{Ba}(\text{Fe}_{1-x}\text{Ru}_x\text{As})_2$ as well as E_F and

v_F of the Dirac cone states determined in the present experiments.

We investigated the effect of Ru doping in iron pnictide superconductor $\text{Ba}(\text{Fe}_{1-x}\text{Ru}_x\text{As})_2$ on MR. Linearly B -dependent MRs were observed below the structure and magnetic transition temperature (T_S), and in the high B regime, a normal state was observed for $x = 0-0.244$, which is consistent with the quantum limit behavior of MR in the Dirac cone states. B^* values estimated for $x = 0-0.150$ were explained in terms of the Landau level splitting for Dirac cone states. Thus, we concluded that the Dirac cone states in Fe pnictides remain after substitution of Fe with Ru and are present in the electronic phase diagram where antiferromagnetism and superconductivity coexist.

The authors are grateful to P. Richard for useful comments. The research was partially supported by Scientific Research on Priority Areas of New Materials Science using Regulated Nano Spaces, the Ministry of Education, Science, Sports and Culture, Grant in Aid for Science, and Technology of Japan. The work was partly supported by the approval of the Japan Synchrotron Radiation Research Institute (JASRI).

-
- [1] Y. J. Uemura, G. M. Luke, B. J. Sternlieb, J. H. Brewer, J. F. Carolan, W. N. Hardy, R. Kadono, J. R. Kempton, R. F. Kiefl, S. R. Kretzmann, P. Mulhern, T. M. Riseman, D. L. Williams, B. X. Yang, S. Uchida, H. Takagi, J. Gopalakrishnan, A. W. Sleight, M. A. Subramanian, C. L. Chien, M. Z. Cieplak, Gang Xiao, V. Y. Lee, B. W. Statt, C. E. Stronach, W. J. Kossler, and X. H. Yu: Phys. Rev. Lett. **62**, 2317 (1989).
- [2] Y. J. Uemura: Solid State Phys. **126**, 23 (2003).
- [3] L. Merchant, J. Ostrick, R. P. Barber, Jr., and R. C. Dynes: Phys. Rev. B **63**, 134508 (2001).
- [4] O. Yuli, I. Asulin, O. Millo, D. Orgad, L. Iomin, and G. Koren: Phys. Rev. Lett. **101**, 057005 (2008).
- [5] H. Fukuyama, J. Phys. Soc. Jpn. **77** (2008) (Online-News and Comments).
- [6] Y. Ran, F. Wang, H. Zhai, A. Vishwanath, and D. H. Lee: Phys. Rev. B **79**, 014505 (2009).
- [7] T. Morinari, E. Kaneshita, and T. Tohyama: Phys. Rev. Lett. **105**, 037203 (2010).
- [8] P. Richard, K. Nakayama, T. Sato, M. Neupane, Y. M. Xu, J. H. Bowen, G. F. Chen, J. L. Luo, N. L. Wang, X. Dai, Z. Fang, H. Ding, and T. Takahashi: Phys. Rev. Lett. **104**, 137001 (2010).
- [9] N. Harrison and S. E. Sebastian: Phys. Rev. B **80**, 224512 (2009).
- [10] K. K. Huynh, Y. Tanabe, and K. Tanigaki: arXiv:1012.3029.
- [11] J. T. Park, D. S. Inosov, Ch. Niedermayer, G. L. Sun, D. Haug, N. B. Christensen, R. Dinnebie, A. V. Boris, A. J. Drew, L. Schulz, T. Shapoval, U. Wolff, V. Neu, X. Yang, C. T. Lin, B. Keimer, and V. Hinkov: Phys. Rev. Lett. **102**, 117006 (2009).
- [12] H. Fukazawa, T. Yamazaki, K. Kondo, Y. Kohori, N. Takeshita, P. M. Shirage, K. Kihou, K. Miyazawa, H. Kito, H. Eisaki, and A. Iyo: J. Phys. Soc. Jpn. **78** 033704 (2009).
- [13] Y. Laplace, J. Bobroff, F. Rullier-Albenque, D. Colson, and A. Forget: Phys. Rev. B **80**, 140501 (2009).
- [14] M. G. Kim, D. K. Pratt, G. E. Rustan, W. Tian, J. L. Zarestky, A. Thaler, S. L. Budko, P. C. Canfield, R. J. McQueeney, A. Kreyssig, and A. I. Goldman: Phys. Rev. B **83**, 054514 (2011).
- [15] X. L. Qi, T. L. Hughes, S. C. Zhang: Phys. Rev. B **78**, 195424 (2008).
- [16] M. Matusiak, Z. Bukowski, and J. Karpinski: arxiv1102.3198.
- [17] H. H. Kuo, J. H. Chu, S. C. Riggs, L. Y. Peter L. McMahon, K. D. Greve, Y. Yamamoto, J. G. Analytis, I. R. Fisher: arxiv1103.4534.
- [18] A. Thaler, N. Ni, A. Kracher, J. Q. Yan, S. L. Budko, and P. C. Canfield: Phys. Rev. B **82**, 014534 (2010).
- [19] A. A. Abrikosov: Phys. Rev. B **58**, 2788 (1998).
- [20] L. Zhang and D. J. Singh: Phys. Rev. B **79**, 174530 (2009).
- [21] V. Brouet, F. Rullier-Albenque, M. Marsi, B. Mansart, M. Aichhorn, S. Biermann, J. Faure, L. Perfetti, A. Taleb-Ibrahimi, P. Le Fevre, F. Bertran, A. Forget, and D. Colson: Phys. Rev. Lett. **105** 087001 (2010).
- [22] H. Hodovanets, E. D. Mun, A. Thaler, S. L. Budko, and P. C. Canfield: Phys. Rev. B **83**, 094508 (2011).
- [23] M. Matusiak, Z. Bukowski, and J. Karpinski: Phys. Rev. B **81**, 020510 (2010).
- [24] Y. Wang, L. Li, and N. P. Ong: Phys. Rev. B **73**, 024510 (2006).